Steel and Composite Structures, Vol. 3, No. 2 (2003) 97-110
DOI: http://dx.doi.org/10.12989/scs.2003.3.2.097

Behavior of lightweight aggregate concrete-encased composite columns

Abbas M. Al-Shahari†

Department of Civil Engineering, Sana'a University, Sana'a, Yemen

Yasser M. Hunaiti‡ and Bassam Abu Ghazaleh‡

Department of Civil Engineering, University of Jordan, Amman, Jordan

(Received July 10, 2002, Accepted February 20, 2003)

Abstract. An experimental study was conducted to investigate the behavior of eccentric lightweight aggregate concrete-encased composite columns. This study aims at verifying the validity of such type of concrete in composite construction and checking the adequacy of the AISC-LRFD and the British Bridge Code BS 5400 specifications in predicting the column strength. Sixteen full-scale pin ended columns subjected to uniaxial bending about the major axis in symmetrical single curvature were tested.

Key words: columns; composite columns; encased columns; lightweight concrete.

1. Introduction

During the past few decades, several composite columns of different ingredients have been used particularly in the construction of tall buildings. One of the common and popular patterns of such columns is the encased steel profile. This system combines the rigidity and formability of reinforced concrete with the strength and speed of construction associated with structural steel to produce an economic structure. The reason for such sound performance is the mutual resistance of both the concrete and the steel section in the composite columns (Hunaiti 1996). The concrete used for encasing the structural steel section not only increases its strength and stiffness, but also it acts as fireproofing. In recognition of the practicality of such construction technique, most international codes provide provisions for determining the capacity of such columns. Moreover, the ductility and energy absorption capacities as well as the high impact resistance were behind the extensive use of such member in seismic zones.

Concrete-encased composite columns have not received the same level of attention as steel or reinforced concrete columns. Past studies on composite columns have mostly concentrated on short specimens and this lead to methods for calculating their ultimate loads, which may seriously

†Assistant Professor
‡Professor

overestimate the load carrying capacity. In recent years, research on composite columns with steel shapes encased in normal concrete has dealt with the behavior of both short and long columns. Consequently, the physical tests on lightweight concrete seem to be rare in literature.

Reducing the self-weight of a structure is undoubtedly considered an advantage if not a necessity in some cases. Using lightweight concrete is one way of a achieving such reduction. In addition to reducing stresses through the lifetime of the structure, due to using smaller elements, the total weight of materials to be handled during construction is also reduced, which consequently increase productivity. Furthermore, lightweight concrete offers better thermal insulation and better fire protection than ordinary concrete. The Load and Resistance Factor Design (LRFD, 93) permit using structural lightweight concrete for encasing steel profiles, but with a characteristic cylinder compressive strength, f_c', of not less than 28 MPa. Other codes such as the British Standard code of practice for design of composite bridges (BS 5400, 79) does not permit the use of concrete other than ordinary concrete of a density less than 2300 kg/m^3 with a 28-day cube compressive strength, f_{cu}, of not less 25 MPa for concrete-encased sections.

This study is aimed at investigating experimentally the behavior of eccentric lightweight aggregate concrete-encased columns in order to verify the validity of such type of concrete in composite construction and to check the adequacy of the applicable provisions such as the LRFD, and the Bridge Code BS 5400 in predicting the strength of lightweight aggregate concrete-encased composite columns. The study was carried out on sixteen full-scale pin-ended columns subjected to uniaxial bending about the major axis and axial compressive load in symmetrical single curvature. With the aim of comparison, nine of the columns were encased in lightweight aggregate concrete, three in normal concrete, while four were tested as bare steel columns. Emphasis was placed on the failure modes, load-deflection and moment-thrust-curvature relationships as well as bond characteristics, slippage, and cracks in concrete. Comparisons between experimental and design results obtained by LRFD, and BS 5400 provisions will be conducted.

2. Test program

The variables investigated in this study can be summarized as follow:

1. Column height of 2 and 3 meters.
2. The equal end eccentricities of the applied load about the major axis at the column ends were 40 mm and 70 mm.
3. Lightweight aggregate concrete strengths of 20.5, 13.7, and 9.7 MPa, and normal weight concrete with compressive strength of 28.2 MPa were used in the tests.
4. Structural steel ratio to gross column area, A_s / A_g, of 4% and 6%.

All columns were of the same concrete cross-sectional dimensions of 230 × 230 mm, reinforced with 4ϕ 12 mm longitudinal steel corner bars, and lateral ties ϕ 8@140 mm on centers. Material and sectional properties of the column specimens are listed in Table 1 and their geometry is illustrated in Fig. 1. The tests were carried out using the universal testing machine at the structural laboratory of Jordan University of Sciences and Technology. Each column specimen was placed in a vertical position and tested under incremental monotonic loading in a 2000 kN capacity M1000/RD universal testing machine from DARTEC Limited as illustrated in Fig. 2.

The basic materials used to build the full-scale column specimens were lightweight aggregate concrete, normal weight concrete, longitudinal structural steel H-shaped section, deformed longitudinal reinforcing bars, and mild steel lateral ties. All column specimens were cast horizontally inside a formwork made out of 20 mm thick precut pieces of plywood using electrical mixer and compacted

Table 1 Details and properties of column specimens

Group No.	Column No.	Column designation	Concrete encasement				Steel sections			Steel bars			Load eccentricity e_x mm	Effective length KL mm
			Size mm	Type and class	Cube strength f_{cu} MPa	Density kg/m^3	Type	Area A_s mm^2	Yield strength, f_y MPa	Diameter mm	Area A_r mm^2	Yield strength, f_{ry} MPa		
I	1	LA2e7R4	230×230	LWAC-A	20.5	1794	HEA 100	2120	337	12.16	465	459	70	2000
	2	LB2e7R4	230×230	LWAC-B	13.7	1650	HEA 100	2120	337	12.16	465	459	70	2000
	3	BS2e7H10	-	-	-	-	HEA 100	2120	337	12.16	465	459	70	2000
	4	LA2e7R6	230×230	LWAC-A	20.5	1794	HEA 140	3140	307	12.16	465	459	70	2000
	5	NC2e7R6	230×230	NC	28.2	2220	HEA 140	3140	307	12.16	465	459	70	2000
	6	BS2e7H14	-	-	-	-	HEA 140	3140	307	12.16	465	459	70	2000
II	7	LA3e7R4	230×230	LWAC-A	20.5	1794	HEA 100	2120	337	12.16	465	459	70	3000
	8	LB3e7R4	230×230	LWAC-B	13.7	1650	HEA 100	2120	337	12.16	465	459	70	3000
	9	BS3e7H10	-	-	-	-	HEA 100	2120	337	12.16	465	459	70	3000
	10	LA3e7R6	230×230	LWAC-A	20.5	1794	HEA 140	3140	307	12.16	465	459	70	3000
	11	NC3e7R6	230×230	NC	28.2	2220	HEA 140	3140	307	12.16	465	459	70	3000
	12	BS3e7H14	-	-	-	-	HEA 140	3140	307	12.16	465	459	70	3000
III	13	LA3e4R4	230×230	LWAC-A	20.5	1794	HEA 100	2120	337	12.16	465	459	40	3000
	14	LB3e4R4	230×230	LWAC-B	13.7	1650	HEA 100	2120	337	12.16	465	459	40	3000
	15	NC3e4R4	230×230	NC	28.2		HEA 100	2120	337	12.16	465	459	40	3000
IV	16	LC2e4R4	230×230	LWAC-C	9.7	1494	HEA 100	2120	337	12.16	465	459	40	2080

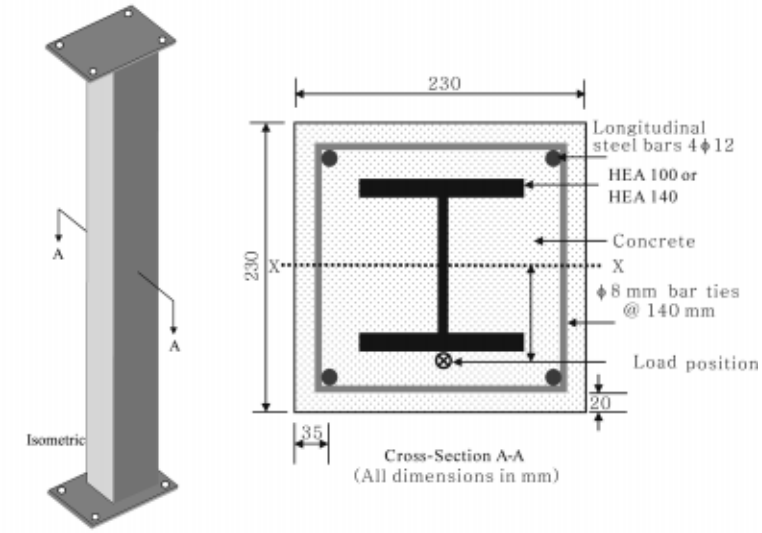

Fig. 1 Column geometry and cross-sectional properties

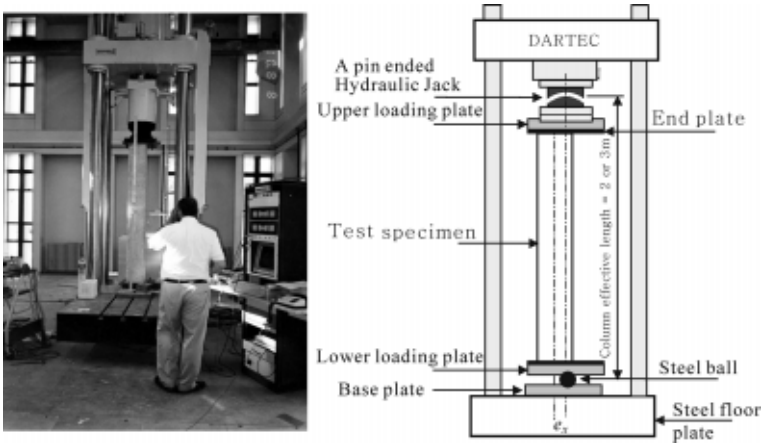

Fig. 2 General view of the testing machine

with a 25 mm vibrator rod. Several trial mixes were attempted on the normal and the lightweight aggregate concrete before obtaining the one that would be the most appropriate with respect to the compressive strength and the density for the final specimens. Concrete mix proportion, average cube strength, slump test results, and concrete density were given in Table 2. Three standard 150 mm cube specimens were taken from each concrete mix, and tested for compression at the time of testing the column specimens in a 1200 kN capacity (M2501 Servo-hydraulic) universal testing machine. Moreover, several tension tests on coupons cut from the H-section were carried out to determine the yield stress of the steel. Some of the coupons were taken from the web others from the flanges. In addition, four stub columns, cut from the H-section of height equals three times their width according to the SSRC (1998) requirements, were tested for compression and their average results are listed in Table 3.

Table 2 Details of concrete mixes

Concrete type	28-d cube strength, f_{cu} average MPa	Average density kg/m^3	Slump test cm	Concrete mix proportions by volume
Lightweight aggregate concrete class A	20.5	1794	12.5	Cement: Sand: Perlite: Pumice 1: 0.5: 1.25: 2 w/c = 0.77
Lightweight aggregate concrete class B	13.7	1650	10.5	Cement: Sand: Perlite: Pumice 1: 0.5: 2: 2.5 w/c = 0.8
Lightweight aggregate concrete class C	9.7	1494	10	Cement: Sand: Perlite: Pumice 1: 0.45: 2: 2.55 w/c = 0.83
Normal weight concrete	28.2	2220	12	Cement: Sand: Aggregate 1: 1.5: 2.5 w/c = 0.6

Table 3 Details of structural steel and reinforcing bars

Type of Steel	A_s mm^2	d mm	t_w mm	b_f mm	t_f mm	Weight kg/m	I_x mm^4 $\times 10^4$	r_x mm	Z_x mm^3 $\times 10^3$	I_y mm^4 $\times 10^4$	r_y mm	Z_y mm^3 $\times 10^3$	f_y MPa	ε_y %
HEA 100	2120	96	5.0	100	8	16.7	349	40.6	83	134	25.1	42.7	337	0.168
HEA 140	3140	133	5.5	140	8.5	24.7	1030	57.3	119	389	35.2	86.4	307	0.154
Reinforcing bars	Diameter = 12.16 mm, A_r = 464.5 mm^2 (4 bars), f_{ry} = 459 MPa, ε_{ry} = 0. 229%													

2.1. Instrumentation and experimental data acquisition

Deflections at the mid height in the direction of the major axis were measured by a dial gauge of 0.01 mm precision, while in the direction of the minor axis were measured by means of a Linear Variable Displacement Transducer (LVDT). Axial deformations against the applied load were recorded and plotted on the X-Y plotter of the DARTEC testing machine.

Concrete strains were evaluated by means of two linear variable displacement transducers (LVDTs) centered vertically at mid-height of compression and tension faces of each specimen with a gauge length of 250 mm as shown in Fig. 3. Four electrical strain gauges were used, one at each of the four flange tips of the H-section at mid-height of column 16 as shown in Fig. 4. For the other fifteen columns two strain gauges were attached at the center of each flange of the H-section also at the column mid-height.

Crack growth on the tension side of the concrete cover was also monitored during the tests. Separation between the column end plates and the attached concrete was also noticed to monitor any localized loss of bond between the two materials. In addition, failure modes were observed and recorded during each test.

2.2. Experimental procedure

The load was applied eccentrically to cause bending about the major axis in single curvature (equal

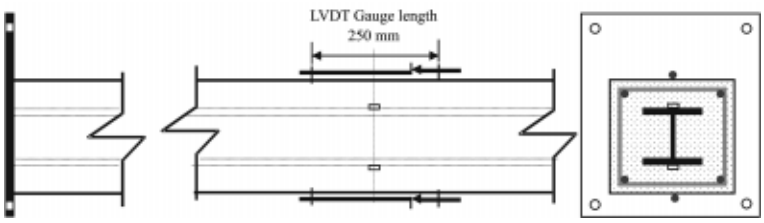

Fig. 3 Locations of electrical strains gauges and LVDTs

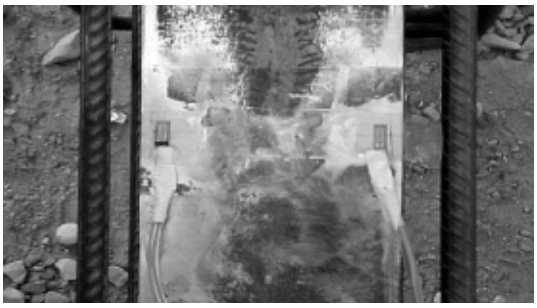

Fig. 4 Electrical strain gauges attached to the flange tips of the *h*-steel section for column 16 (Before casting concrete)

ends eccentricity). Each one of the column specimens was loaded continuously by a 2000 kN capacity universal testing machine and observations were made at each load stage to detect the initiation of any visible cracks on the tensile faces of the specimen, or concrete spall-off or buckling of the reinforcing bars. Values of the applied load against lateral displacements were recorded digitally during testing, while, strains, and LVDTs readings were collected by the data acquisition system. Loading rate was either 0.5 or 0.7 kN/sec up to about 80% of expected failure load, and then the mode of loading was changed to displacement control with a displacement rate of 0.01 mm/sec. The test was terminated when the reinforcing bars had been buckled and the spall of concrete cover had taken place whereas the load decreased to about 80-70% of its ultimate value.

3. Test results and discussion

Experimental observations of the tested specimens and recorded data are utilized in this section to explain and describe the behavior of lightweight concrete-encased columns subjected to axial load and equal end moments about the major axis.

3.1. Failure modes of column specimens

The type of failure mode observed for all composite column specimens during testing was typically that of crushing of concrete on the compression face of the column with some noticeable cracking on the tensile face. The first stage always corresponds to yielding in the compression flange of the H-section. The strain in the steel flange at the tensile zone was next to reach yielding. A continuous deterioration in column stiffness was observed. Final collapse was accompanied by spalling of concrete in the compression zone as shown in Fig. 5. This immediately resulted in buckling between ties of the

Fig. 5 Failure mode of columns 11 and 16

longitudinal reinforcement bars at the compression corners, reducing the column to a mechanism. Steel columns failed due to yielding in the compression flange of the H-section and strains in the steel flange at the tension zone was next to reach yield. The first sign of damage to concrete occurred at loads not less than 95% of the failure load in all the tests. Serious spalling and crushing of concrete lumps always occurred at, or beyond, failure loads.

It was expected that severe damage due to failure will occur at mid-height in all columns because all columns were tested in single curvature, i.e., equal end eccentricities. Some specimens showed different behavior, that is; failure took place near the bottom end plate of the column. This premature crushing of the concrete near the bottom end plate is possibly due to a misalignment of the top and bottom eccentricities that could have created an unsymmetrical pinned-ended condition. Furthermore, whatever the reason for this type of failure it had no adverse effect on the load-carrying capacity of these columns.

3.2. Load carrying capacity

The experimental failure loads of the tested columns are given in Table 4 and are compared with the predicted loads, as calculated by the LRFD, and the BS 5400. Although no material safety factors were taken into account in the calculations, the experimental failure loads were always well in excess of the estimated values. A careful examination of Table 4 shows the following:

1. The design provisions of the present code procedure LRFD as well as BS 5400 are found to be adequate to predict the strength of lightweight aggregate concrete-encased composite columns.
2. The predicted column strengths using these two methods are on the conservative side and are in reasonable agreement with the test results. The average ratio of the ultimate load capacity obtained by AISC-LRFD Code to the experimental load carrying capacity ($P_{LRFD} / N_e = 0.726$) is nearly the same or slightly lower than that obtained by Bridge Code BS 5400 ($N_{BS} / N_e = 0.731$).
3. The load carrying capacity of the bare steel section increased by the concrete encasement by about 265% for LWAC class A and 230% for LWAC class B, as indicated by comparing columns 1, 2, 3, 7, 8, and 9 in Table 4.
4. The load carrying capacity is inversely proportional to the eccentricity of the applied load as indicated by comparing columns 13, 14, and 15 of 40 mm eccentricity with columns 7 and 8 of 70 mm eccentricity. The load carrying capacity of columns 13 and 14 was 127% on average of that of columns 7 and 8.

Table 4 Test results of columns

Group No.	Column No. and designation	Load eccentricity about major axis e_x mm	Average concrete cube strength and Unit weight f_{cu}- w_c MPa-kg/m^3	Experimental			AISC-LRFD				Bridge Code BS 5400				
				Failure load N_e kN	Mid- height deflection at failure about major axis u mm	Mid-height moment at failure M_{uxe} kN.m	Ultimate load P_{LRFD} kN	Nominal load P_{no} kN	Ultimate moment of resistance M_{nx} kN.m	$\frac{P_{LRFD}}{N_e}$ Average (0.726)	Ultimate load N_{BS} kN	Squash load N_u kN	Concrete contribution factor a_c	Ultimate moment of resistance M_{ux} kN.m	$\frac{N_{BS}}{N_e}$ Average (0.731)
I	1LA2e7R4	70	20.5-1794	654	8.13	51.1	487.5	1358.8	53.9	0.75	512.9	1618.7	0.427	55.7	0.78
	2LB2e7R4	70	13.7-1650	558	7.04	43.0	453.5	1194.6	51.8	0.81	470.9	1389.5	0.332	57.8	0.84
	3BS2e7H10	70	-	248	18.2	21.9	188.3	714.4	27.8	0.76	182.0	714.4	-	28.0	0.73
	4LA2e7R6	70	20.5-1794	962	8.15	75.2	670.8	1598.3	82.4	0.70	675.9	1854.3	0.365	81.5	0.70
	5NC2e7R6	70	28.2-2220	949	8.85	74.8	715.0	178.5	84.6	0.75	789.3	2108.6	0.442	91.9	0.83
	6BS2e7H14	70	-	417	10.02	33.4	366.5	964	53.11	0.88	336.7	964.0	-	53.1	0.81
II	7LA3e7R4	70	20.5-1794	641	11.98	52.6	443.0	1358.8	53.9	0.69	448.6	1618.7	0.427	55.7	0.70
	8LB3e7R4	70	13.7-1650	554	14.2	46.7	412.8	1194.6	51.8	0.75	421.2	1389.5	0.332	57.8	0.76
	9BS3e7H10	70	-	240	35.35	25.3	127.9	714.4	27.8	0.53	134.4	714.4	-	28.0	0.56
	10LA3e7R6	70	20.5-1794	895	17.0	77.9	612.0	1598.3	82.4	0.68	588.8	1854.3	0.365	81.5	0.66
	11NC3e7R6	70	28.2-2220	900	19.95	81.0	653.0	178.5	84.6	0.73	671.5	2108.6	0.442	91.9	0.75
	12BS3e7H4	70	-	404	31.0	40.8	290.5	964	53.11	0.72	278.0	964.0	-	53.1	0.69
III	13LA3e4R4	40	20.5-1794	813	15.8	45.4	581.5	1358.8	53.9	0.72	591.1	1618.7	0.427	55.7	0.73
	14LB3e4R4	40	13.7-1650	704	9.51	34.9	537.0	1194.6	51.8	0.76	538.7	1389.5	0.332	57.8	0.77
	15NC3e4R4	40	28.2-2220	1115	17.3	63.9	631.5	1544.8	54.98	0.57	664.2	1878.3	0.506	58.6	0.60
IV	16LC2e4R4	40	9.7-1494	680	5.4	30.9	556.5	1098	49.3	0.82	538.0	1254.7	0.261	52.8	0.79

$M_{xe} = N_e(e_x+u)$

5. The effect of column height on the load carrying capacity was very small as indicted by comparing columns 7 and 8 of 3 m height to columns 1 and 2 of 2 m height.
6. The effect of steel ratio on the load carrying capacity of the composite column was significant, where 2% increase in steel ratio causes an increase in the load carrying capacity by about 47% as indicated by comparing columns 1 and 4, and was about 40% for columns 7 and 10.
7. The strength of the column encased in lightweight aggregate class "A" reaches 73% and class "B" reaches 63% of the strength of columns encased in normal concrete as in the case of columns 13, 14, and 15.

3.3. Strains

The load-strain response was recorded during the tests for all column specimens in steel and concrete at the columns mid-height. Load-strain curves of columns 1, 6, 11, and 13 are illustrated in Fig. 6. Strains for the rest of the columns are similar to those presented in Fig. 6. The steel yield strains which were obtained from the coupon tensile tests (Table 2) varied between 0.154 % and 0.17% and the concrete ultimate strains were between 0.25% and 0.4%. None of the tested columns that failed at the mid-height reached the yield strain at loads less than 95% of the failure load. It can be seen from the load-strain results for columns 3, 6, 9, 11, 12, 13, 14, 15, and 16, which failed at the mid-height, that the strains reached the yield strain and the ultimate concrete strain at compression side, while the strains in the steel flange at the tension zone was next to reach yielding. In addition, for all columns, none of the tension steel flanges reached the yield strain at failure, this is possibly due to the low moment compared to the axial load.

The composite action was also confirmed by plotting the strains measured in steel and concrete across the column section at the mid-height. Strain distribution at the mid-height section of columns 1, 6, and 11, at several load levels, are shown in Fig. 7. The linear strain distribution across the section was maintained up to over 90% of the failure load, above which the strain in steel and concrete did not

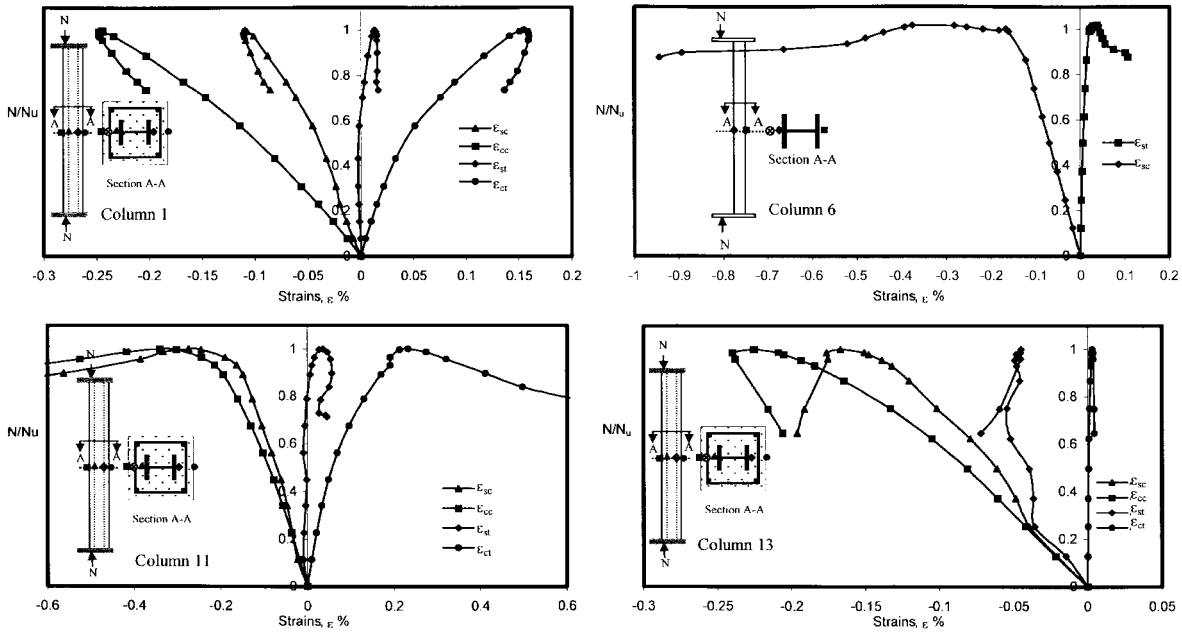

Fig. 6 Strains in steel and concrete at mid-height of columns 1, 6, 11, and 13

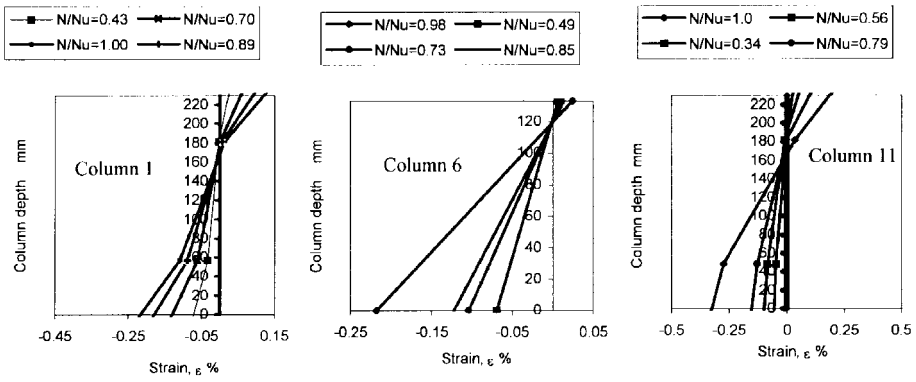

Fig. 7 Mid-height strain distribution across the section at different N/N_u, ratios for columns 1, 6, and 11

exhibit similar linear relationships. Strain distribution for the rest of the columns are similar to those presented in Fig. 7.

3.4. Lateral deflections

Lateral deflections in the directions of the major and the minor axes at mid-height of columns 4, 5, 6, 10, 11, and 12 were plotted against the applied load as shown in Fig 8. All columns were tested under major axis bending and showed very small deflections in the minor axis direction especially for concrete-encased columns. These deflections were very small and started to increase at loads more than 90% of the failure load for bare steel columns, while for concrete-encased columns, started to increase beyond failure load. For lightweight aggregate concrete-encased columns, the deflections about the major axis were very small at low loads and started to increase at loads between 20 and 30% of the failure load. It can be seen from the figures, that columns encased in lightweight aggregate concrete exhibited less lateral deflection than those incased in normal concrete and the bare steel columns. The steel ratio has insignificant effect on the lateral deflections for columns of steel ratio of 4% and for columns of steel ratio of 6%. The effect of column height was significant, longer columns exhibited more deformations. Lateral deflections for the rest of the columns are similar to those presented in Fig. 8.

3.5. Axial shortening

The load-axial shortening results were recorded for columns 7, 8, 9, 13, 14, 15, and 16, and these are illustrated for both LWAC and normal concrete-encased columns in addition to the bare steel columns in Fig. 9. The load-axial shortening curves were used in ascertaining the onset of yielding of each test, together with the determination of the ultimate load of each individual member. It can be seen from the figures that the axial shortening increase slowly with the increase in the load up to failure then it increase faster with the load decrease especially for bare steel columns. Load-axial shortening for the rest of the columns are similar to those presented in Fig. 9.

3.6. Moment-thrust-curvature relationship

The moment-thrust-curvature relationships were determined from the strain distribution across the

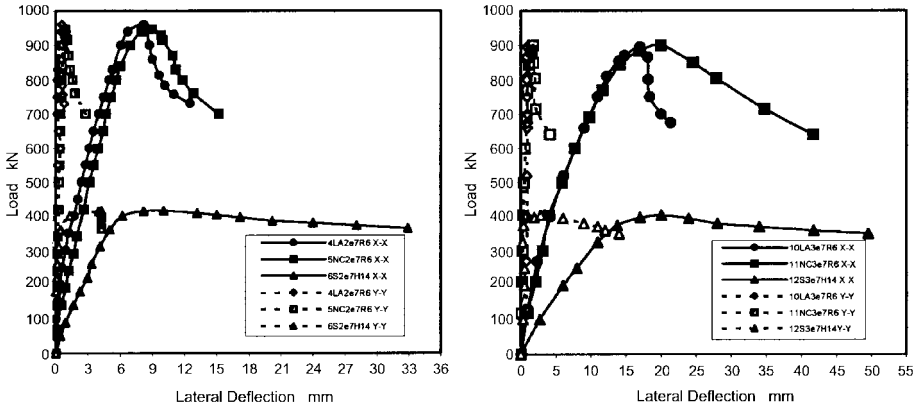

Fig. 8 Load-lateral deflection curves about major and minor axes at mid-height of columns 4, 5, 6, 10, 11, and 12

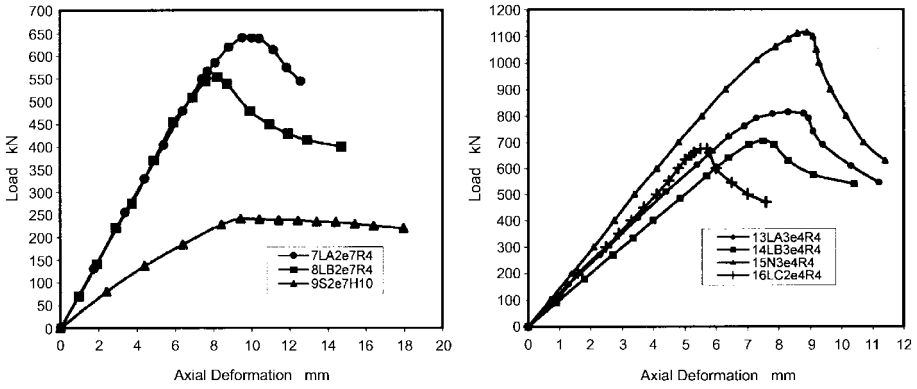

Fig. 9 Load versus axial shortening of columns 7, 8, 9, 13, 14, 15, and 16

column section at mid-height. Plots of the moment-thrust-curvature for columns 7, 8, 9, 13, 14, 15, and 16 are presented in Fig. 10. Moment-thrust-curvature for the rest of the columns are similar to those presented in Fig. 10. The curvature value at each load level was determined by taking the average of the two strain values on each steel flange and concrete strains at the compression and tension faces, as follow:

$$\phi = \frac{\varepsilon_c}{y}$$

and $$y = h\frac{\varepsilon_c}{\varepsilon_c + \varepsilon_t}$$

hence $$\phi = \frac{\varepsilon_c + \varepsilon_c}{h}$$

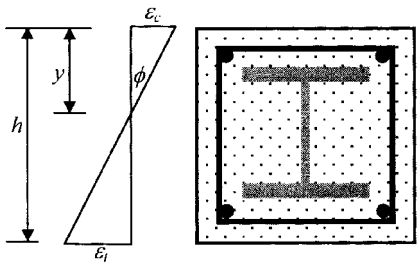

where

ϕ the curvature in radian/mm.
y the distance from extreme fiber to the neutral axis.

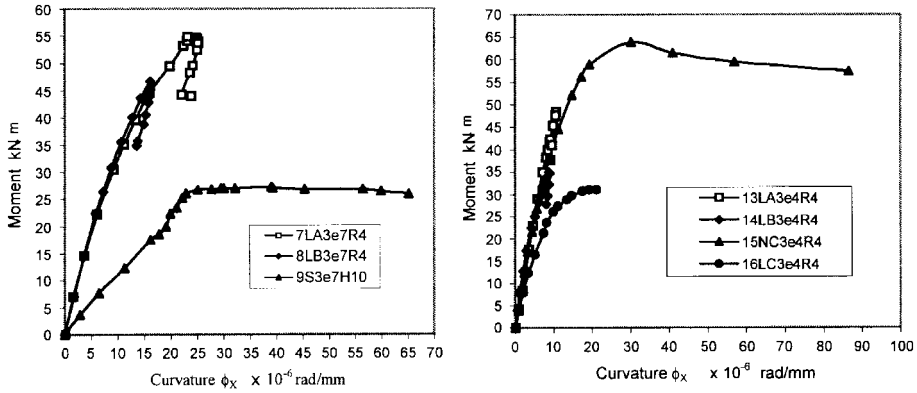

Fig. 10 Moment-thrust-curvature relationship about major axis at mid-height for columns 7, 8, 9, 13, 14, 15, and 16

ε_c strain in most compressed fiber in concrete.
ε_t strain in extreme concrete fiber in tension.
h column overall depth.

The experimental moment, M_x, is given by:

$$M_x = P_e(e_x + u)$$

where

P_e experimental applied load.
e_x eccentricity of the applied load about the major axis.
u deflection due to the applied load.

It can be seen from the curves that the stiffening effect of the lightweight concrete encasement is higher for low eccentricities and as the eccentricity increases, the curvature decreases. This is because as the eccentricity increase a large area of concrete will be subjected to tension and hence cracked, thus causing a reduction in the stiffening effect of the concrete. The increase in steel ratio causes a slight increase in curvature. For the same steel ratio, as the column height increases the curvature increases. Composite columns exhibit less ductility than the bare steel columns. Furthermore, lightweight concrete-encased columns have lower curvature than normal concrete-encased columns as indicated in Fig. 10.

3.7. Separation and bond

Separation between the concrete and the column end plates was observed in some specimens throughout the test especially at high load levels (more than 90% of the failure load). The separation occurred at the tension side and was very small (less than 1 mm) in columns with 40 mm eccentricity and between 1 to 3 mm in columns with 70 mm eccentricity.

3.8. Cracks

It was noticed that cracks developed quite early in the long columns encased by LWAC and subjected

to large eccentricities. However, in no case did the cracks seem to affect the load carrying capacity of the columns. Columns of 2 m height and large eccentricity of 70 mm (columns 1, 2, 4, and 5) showed minor hairline cracks at a load ratio of about 60-70% of the failure load on the tension sides of the specimens. Beyond the maximum load level, major cracks started to appear on the tension sides of the specimens at locations near the middle of the columns. As the axial load started to drop and the lateral displacement increased, concrete on the compression sides of the column started to spall off. Furthermore, columns of 3 m height and large eccentricity of 70 mm (columns 7, 8, 10, and 11) showed minor hairline cracks at a load ratio of about 50-60% of the failure load on the tension sides of the specimens. Signs of concrete crushing started to appear on the compression sides of the specimens at a load level near the maximum load. In addition, for columns encased in lightweight aggregate concrete with 3 m height and low eccentricity of 40 mm, cracks were observed at load ratio of 70-75% of the failure load as in columns 13, 14, 15, and 16.

4. Conclusions

The test results have shown that lightweight concrete encasement significantly enhances the load carrying capacity of the steel sections but its ductility is decreased. Furthermore, lightweight concrete columns of small load eccentricity, reached between 63% and 73% of the load carrying capacity of normal concrete columns, while for large eccentricity, the capacities are almost identical. Moreover, lightweight concrete can provide perfect bond to steel sections up to failure. The structural steel ratio to gross column area has also a significant effect on the load carrying capacity of the composite column. A change in steel ratio from 4% to 6% causes an increase in the load carrying capacity that reached 47%. It is also demonstrated that, the design provisions of the present code procedures; LRFD as well as BS 5400 are found to be adequate to predict the strength of lightweight concrete-encased composite columns. Column strength predictions using these two methods are on the conservative side and are in reasonable agreement with the test results. Although quality control of lightweight aggregate concrete is somewhat difficult, it is still valuable in certain cases to replace ordinary concrete by lightweight aggregate concrete due to its good performance and distinct advantages.

References

Al-Shahari, A. (2002), "Behavior of lightweight concrete-encased composite columns", Ph. D. Thesis, University of Jordan, Amman, Jordan.

American Institute of Steel Construction (1993), Load and Resistance Factor Design Specification for Structural Steel Buildings (AISC-LRFD). Chicago, Illinois.

European Committee for Standardization. (Eurocode 4) (1992), Design of Composite Steel and Concrete Structures-Part 1: General Rules and Rules for Building, Brussels, Belgium.

Furlong R.W. (1988), Steel-Concrete Composite Columns II. In: Narayanan R. (editor), *Steel-Concrete Composite Structures: Stability and Strength*, Elsevier Applied Science Publishers LTD, London.

Hunaiti, Y. M. (1996), "Composite actions of foamed and lightweight aggregate concrete", *Journal of Materials in Civil Engineering*, ASCE, **8**(3): 111-113.

Hunaiti, Y. M. (1997), "Strength of composite sections with foamed and lightweight concrete", *J. Mater. in Civil Eng.*, ASCE, **9**(2): 58-61.

Neville, A. M. (2000), *Properties of Concrete*. 4th. edition, Prentice Hall, London.

SSRC (1998), Composite Columns and Structural Systems. In: Galambos, T. V. (editor), *Guide to Stability*

Design Criteria for Metal Structures. 5th edition. John Wiley & Sons, Inc. New York.
Saw, H. S. and Liew, J. R. (2000), "Assessment of Current methods for the design of composite columns in buildings", *Journal of Constructional Steel Research*, 53:121-147.
Shakir-Khalil, H. (1988), Steel-Concrete Composite Columns I. In: Narayanan R. (editor), *Steel-Concrete Composite Structures: Stability and Strength*, Elsevier Applied Science Publishers LTD, London.
Sharif, R. L. (1988), "The use of pozzolans for lightweight concrete in jordan", *Dirasat, J. Pure and Appl. Sciences*, University of Jordan, XV(6): 94-111.
Smith, D. G. E. (1980), "Composite columns with lightweight concrete casing", *The Structural Engineer*, **58A**(8): 246-248.
Videla, C. and Lüpez, M. (2000), "Mixture proportioning methodology for structural sand lightweight concrete", *ACI Materials Journal*, **97**(3), May-June: 281-289.
Virdi, K. S. And Dowling, P. J. (1973), "The ultimate strength of composite columns in biaxial bending", *Proc. Instn. Civil Engineers*, Part 2, 55, Mar. 251-272.

Notation

A_r : area of longitudinal reinforcement
A_s : area of the steel shape
b_f : breadth of steel flange of H-section
d : overall depth of the H-section
e_x : eccentricity of the applied load about the major axis
f_{cu} : characteristic 28-day cube compressive strength of concrete
f_{ry} : nominal yield strength of reinforcement
f_y : yield strength of steel shape
f_c' : concrete cylinder compressive strength
h : column overall depth
I : moment of inertia of the steel shape
M_u : required flexural strength (LRFD-C1)
M_u : ultimate moment of resistance (BS 5400)
M_{uxe} : experimental mid-height moment about the major axis at failure
M_{xe} : experimental mid-height moment about the major axis
N_{BS} : ultimate load predicted by BS 5400
N_e : experimental failure load
N_u : squash load
P_e : experimental applied load
P_{LRFD} : ultimate load predicted by LRFD
P_{no} : nominal axial strength of stub column (LRFD)
r : radius of gyration of the steel shape
t_f : average thickness of the flange of a steel section
t_w : average thickness of the web of a steel section
u : experimental mid-height deflection about the major axis
x : subscript relating symbol to strong axis bending
y : subscript relating symbol to weak axis bending, or the distance from extreme fiber to the neutral axis
Z : plastic section modulus of the steel section
ε_c or ε_{cc} : strain in most compressed fiber in concrete
ε_t or ε_{ct} : strain in extreme concrete fiber in tension
ε_{sc} : strain in most compressed fiber in steel
ε_y : yield strain of steel
ε_{ry} : yield strain of reinforcement
α_c : concrete contribution factor

CC